Available online at www.sciencedirect.com

ScienceDirect

IFAC Papers Online CONFERENCE PAPER ARCHIVE

IFAC PapersOnLine 55-36 (2022) 109–114

Suppression of axial-torsional vibrations of a distributed drilling system by the eigenvector contradiction method

Mohammad Amin Faghihi * **Shabnam Tashakori** **,***,**** **Ehsan Azadi Yazdi** * **Mohammad Eghtesad** * **Nathan van de Wouw** †

* *Department of Mechanical Engineering, Shiraz University, Iran*
** *Centre for Applied Dynamics Research, School of Engineering, University of Aberdeen, United Kingdom*
*** *Department of Mechanical and Aerospace Engineering, Shiraz University of Technology, Iran*
**** *Rahesh Innovation Center, Iran*
† *Department of Mechanical Engineering, Eindhoven University of Technology, 5600 MB Eindhoven, The Netherlands*

Abstract: This article proposes an active control strategy to suppress self-excited coupled axial-torsional vibrations of a distributed drill-string system while the coupling takes place through the bit-rock interaction. The drill-string model is expressed as Neutral-type Delay Differential Equations (NDDEs) with constant and state-dependent state delays and constant input delays. As a first step in the novel controller design, an implementable input transformation is introduced, resulting in the elimination of the neutral terms from the equations of motion. This supports a simplified next step of stabilizing controller design. In the second step, a new analytic method named the "Eigenvector Contradiction Method" is proposed to provide sufficient conditions to ensure that all eigenvalues have real parts less than a prescribed value. Based on this criterion, an automated parametric feedback control law is designed. A case study simulation is presented to illustrate the effectiveness of the proposed control strategy.

Keywords: Distributed drill-string; Coupled axial-torsional vibrations; Neutral-type Time-Delay (NTD) model; State-dependent delay; Input delay.

1. INTRODUCTION

Drill-string systems suffer from self-excited oscillations leading to drilling efficiency reduction and system failure. The interaction forces between formation and Polycrystalline Diamond Compact (PDC) bits consist of a cutting and a frictional contact process Detournay and Defourny (1992). Regenerative cutting effects are known as the root cause of self-excited oscillations in drilling systems Richard et al. (2007); Aarsnes and van de Wouw (2018).

Several approaches have been employed to model the drill-string dynamics: lumped-parameter models Germay et al. (2009); Tashakori and Fakhar (2019); Richard et al. (2007), finite element models Priest et al. (2021), distributed parameter models Aarsnes and van de Wouw (2018), and Neutral-type Time Delay (NTD) models Boussaada et al. (2012); Tashakori et al. (2020); Faghihi et al. (2022). The NTD model is more comprehensive than lumped-parameter models, and easier to analyze compared to models based on Partial Differential Equations (PDEs) Krstic (2009).

Various approaches have been proposed to suppress unwanted axial-torsional drill-string vibrations for lumped-parameter models Besselink et al. (2015), for finite element models Vromen et al. (2017), for distributed parameter models Bresch-Pietri and Di Meglio (2016), and for NTD models Saldivar et al. (2013); Tashakori et al. (2021). However, existing control solutions for the suppression of coupled axial-torsional vibrations in the framework of NTD models have some drawbacks/limitations. The considered bit-rock interaction law in Saldivar et al. (2013) does not capture the regenerative effects. The proposed controller in Tashakori et al. (2021) is not automated, i.e., the controller design should be repeated if the drill-string parameter values change.

In this paper, the infinite-dimensional drill-string dynamics is formulated in terms of Neutral-type Delay Differential Equations (NDDEs) with multiple constant or state-dependent state and input delays. The lateral vibration is neglected, while the axial and torsional motions are coupled through the bit-rock interaction. One of the main challenges towards controlling the systems with NDDE open-loop dynamics is the existence of spectral asymptotes which cannot be changed by state-feedback controllers Loiseau et al. (2002). By introducing an implementable input-transformation, i.e., precompensator, the dynamics is transformed into simpler Retarded Delay Differential Equations (RDDEs). Herein, a new approach is developed by presenting a sufficient condition to ensure that all

10.1016/j.ifacol.2022.11.342

eigenvalues have real values less than a prescribed value. In Tashakori et al. (2021), an observer-like predictor was developed to compensate for the input delays. Hence, this paper focuses on designing a novel state-feedback controller assuming that the predicted states are available. The automated parametric structure of the controller makes it easily applicable for different drill-string systems with different parameter values.

2. DRILL-STRING MODEL

The equations governing the torsional and axial dynamics of the drill-string are given by Aarsnes and van de Wouw (2018); Tashakori et al. (2020):

$$\frac{\partial^2\Phi}{\partial x^2}(x,t) = c_t^2\frac{\partial^2\Phi}{\partial t^2}(x,t),\ \frac{\partial^2 U}{\partial x^2}(x,t) = c_a^2\frac{\partial^2 U}{\partial t^2}(x,t), \quad (1)$$

which are wave equations with $\Phi(x,t)$ and $U(x,t)$, respectively, the angular and axial displacements of the cross section located at the (axial) distance x from the top extremity of the drill-string at time t. In addition, the wave constants in (1), c_t and c_a, are defined as $c_a = \sqrt{\rho/E}$, $c_t = \sqrt{\rho/G}$, where ρ, E, and G are, respectively, the density, Young's modulus, and the shear modulus of the pipes. Employing Riemann variables, the solution of (1) is defined as follows:

$$\Phi(x,t) = \eta_t(t + c_t x) + \xi_t(t - c_t x), \quad (2a)$$
$$U(x,t) = \eta_a(t + c_a x) + \xi_a(t - c_a x), \quad (2b)$$

where η and ξ are, respectively, associated to the up- and down-traveling waves with the subscripts t and a relating to the torsional and axial dynamics. Differentiating (2a) with respect to t and x gives:

$$\frac{\partial\Phi}{\partial t}(0,t) = \dot\eta_t(t) + \dot\xi_t(t), \quad (3a)$$
$$\frac{\partial\Phi}{\partial x}(0,t) = c_t\dot\eta_t(t) - c_t\dot\xi_t(t), \quad (3b)$$
$$\frac{\partial\Phi}{\partial t}(L,t) = \dot\eta_t(t+\tau_t) + \dot\xi_t(t-\tau_t), \quad (3c)$$
$$\frac{\partial\Phi}{\partial x}(L,t) = c_t\dot\eta_t(t+\tau_t) - c_t\dot\xi_t(t-\tau_t), \quad (3d)$$

where L is the length of the string and $\dot F(t)$ denotes the differentiation of $F(t)$ with respect to t and the time-delay $\tau_t = c_t L$ is the time required for the torsional waves to travel from one end of the string to the other.

The equations of motion of the Bottom Hole Assembly (BHA), which is considered as a rigid part, are as follows:

$$J_b\ddot\Phi_b = -GJ\frac{\partial\Phi}{\partial x}(L,t) - T(t), \quad (4a)$$
$$M_b\ddot U_b = -EA\frac{\partial U}{\partial x}(L,t) - W(t), \quad (4b)$$

where $\Phi_b(t) = \Phi(L,t)$ and $U_b(t) = U(L,t)$ represent the BHA angular and axial dislacements, respectively. J is the cross-sectional polar moment of area, A is the cross-sectional area of the string, J_b is the BHA moment of inertia, and M_b is the mass of the BHA. Furthermore, $T(t)$ and $W(t)$ are the applied Torque On Bit (TOB) and Weight On Bit (WOB) from the formation, respectively.

The torsional dynamics can be obtained by solving (3) and (4a) as a set of algebraic equations (for more details refer to Tashakori et al. (2021)):

$$\ddot\Phi_b(t) - \ddot\Phi_b(t-2\tau_t) = -\frac{GJc_T}{J_b}\big(\dot\Phi_b(t) + \dot\Phi_b(t-2\tau_t)\big) + \frac{1}{J_b}\big(-T(t) + T(t-2\tau_t)\big) + \frac{2GJc_t}{J_b}\Omega(t-\tau_t), \quad (5)$$

where $\Omega(t)$ is the rotary table angular velocity. The axial dynamics can be obtained in a similar way yielding:

$$\ddot U_b(t) - \ddot U_b(t-2\tau_a) = -\frac{EAc_a}{M_b}\big(\dot U_b(t) + \dot U_b(t-2\tau_a)\big) + \frac{1}{M_b}\big(-W(t) + W(t-2\tau_a)\big) + \frac{2EAc_a}{M_b}V(t-\tau_a), \quad (6)$$

where $V(t)$ is the imposed axial velocity at the top-side of the drill-string. $V(t)$ and $\Omega(t)$ are considered as the control inputs. The time delay $\tau_a = c_a L$ is the time required for the axial waves to travel the drill-string length. The following bit–rock interaction law is employed to model $T(t)$ and $W(t)$ Richard et al. (2007):

$$T(t) = T_c(t) + T_f(t), \quad (7a)$$
$$W(t) = W_c(t) + W_f(t), \quad (7b)$$

where $T(t)$ and $W(t)$ are composed of the cutting and wearflat/frictional components, denoted with c and f subscripts, respectively. In the case of low-amplitude vibrations around the nominal solution, the wearflat/frictional components are constant and the cutting components are defined as follows [1] Detournay and Defourny (1992):

$$T_c(t) = \frac{1}{2}\epsilon a^2 d(t), \quad W_c(t) = \epsilon a\zeta d(t), \quad (8)$$

where ϵ is the rock intrinsic specific energy, a is the bit radius, and ζ is the cutter inclination number. Furthermore, $d(t)$, the depth of cut, is governed by:

$$d(t) = n\big(U_b(t) - U_b\big(t - \tau_n(t)\big)\big), \quad (9a)$$
$$\Phi_b(t) - \Phi_b\big(t - \tau_n(t)\big) = 2\pi/n. \quad (9b)$$

where n is the number of the cutting blade, and $\tau_n(t)$ is a state-dependent time delay governed by (9b). Now, the total model is defined by (5)-(9b) that it is an NDDE with constant and state-dependent state delays and constant input delays.

2.1 Perturbation Dynamics

The steady-state response of the bit to constant imposed velocities at the surface, V_0 and Ω_0, with initial conditions Φ_0 and U_0, is given by:

$$\Phi_{b_s}(t) = \Omega_0 t + \Phi_0, \quad U_{b_s}(t) = V_0 t + U_0. \quad (10)$$

The perturbed variables associated with the steady-state response are defined as follows:

$$A(t) = A_s(t) + A_p(t), \quad B(t) = B_0 + B_p(t), \quad (11)$$

where $A \in \{\Phi_b, U_b\}$ and $B \in \{\Omega, V, T, W, d\}$ with the subscripts 0 and p correspond to nominal and perturbed responses, respectively (for more details refer to Tashakori et al. (2021)). According to the low amplitude vibration assumption, only the cutting components of the bit-rock interaction contribute to the perturbed part of the TOB and WOB as follows:

$$T_p(t) = \frac{1}{2}\epsilon a^2 d_p(t), \quad W_p(t) = \epsilon a^2 d_p(t). \quad (12)$$

Regarding (12) and considering that the perturbed response (as well as the nominal response) satisfies (5) and

[1] for more general cases with high vibration amplitudes see Tashakori et al. (2021)

(6), the equations of motion in the perturbed coordinates are obtained as follows:

$$\ddot{\Phi}_{b_p}(t) - \ddot{\Phi}_{b_p}(t-2\tau_t) = -\frac{GJc_T}{J_b}\big(\dot{\Phi}_{b_p}(t) + \dot{\Phi}_{b_p}(t-2\tau_t)\big) - \frac{\epsilon a^2}{2J_b}\big(d_p(t) - d_p(t-2\tau_t)\big) + \frac{2GJc_t}{J_b}\Omega(t-\tau_t), \quad (13a)$$

$$\ddot{U}_{b_p}(t) - \ddot{U}_{b_p}(t-2\tau_a) = -\frac{EAc_a}{M_b}\big(\dot{U}_{b_p}(t) + \dot{U}_{b_p}(t-2\tau_a)\big) - \frac{\epsilon a\zeta}{M_b}\big(d_p(t) - d_p(t-2\tau_a)\big) + \frac{2EAc_a}{M_b}V(t-\tau_a). \quad (13b)$$

The only nonlinear term in (13a) and (13b) is the term related to the perturbed depth of cut $d_p(t)$, which, after linearization is given by Tashakori et al. (2021):

$$d_p(t) = n\big(U_{b_p}(t) - U_{b_p}(t-\tau_0) - \frac{V_0}{\Omega_0}(\Phi_p(t) - \Phi_p(t-\tau_0))\big), \quad (14)$$

with $\tau_0 = \frac{2\pi}{n\Omega_0}$.

2.2 Dimensionless equations of motion

The characteristic time and length, the dimensionless angular and axial displacements, and the dimensionless control inputs are introduced as follows:

$$t_* = \frac{J_b}{GJc_t}, \quad L_* = \frac{2J_b}{nt_*^2\epsilon a^2}, \quad \phi = \Phi_{b_p}, \quad u = \frac{U_{b_p}}{L_*},$$
$$\omega(\hat{t}) = \frac{2GJc_t}{J_b}t_*^2\Omega(t), \quad v(\hat{t}) = \frac{2EAc_a}{M_b}\frac{t_*^2}{L_*}V(t), \quad (15)$$

with $\hat{t} = t/t_*$ the dimensionless time. The dimensionless form of (13) is hence given by:

$$\phi''(\hat{t}) - \phi''(\hat{t}-2\hat{\tau}_t) = -\phi'(\hat{t}) - \phi'(\hat{t}-2\hat{\tau}_t) - \hat{d}(\hat{t}) + \hat{d}(\hat{t}-2\hat{\tau}_t) + \omega(\hat{t}-\hat{\tau}_t), \quad (16a)$$

$$u''(\hat{t}) - u''(\hat{t}-2\hat{\tau}_a) = -\kappa u'(\hat{t}) + \kappa u'(\hat{t}-2\hat{\tau}_a) - \psi\hat{d}(\hat{t}) + \psi\hat{d}(\hat{t}-2\hat{\tau}_a) + v(\hat{t}-\hat{\tau}_a), \quad (16b)$$

with the dimensionless time-delays $\hat{\tau}_t = \tau_t/t_*$, $\hat{\tau}_a = \tau_a/t_*$, $\hat{\tau}_0 = \tau_0/t_*$, dimensionless parameters

$$\chi = \frac{nV_0\epsilon a^2}{2J_b\Omega_0}t_*^2, \quad \kappa = \frac{EAc_a}{M_b}t_*, \quad \psi = \frac{n\epsilon a\zeta}{M_b}t_*^2, \quad (17)$$

and the dimensionless form of the linearized perturbed depth of cut:

$$\hat{d}(\hat{t}) = \big(u(\hat{t}) - u(\hat{t}-\hat{\tau}_0)\big) - \chi\big(\phi(\hat{t}) - \phi(\hat{t}-\hat{\tau}_0)\big) := \int_{\hat{t}-\hat{\tau}_0}^{\hat{t}} \Big(u'(\theta) - \chi\phi'(\theta)\Big)d\theta. \quad (18)$$

By employing the dimensionless angular and axial velocities and the dimensionless depth of cut as representative states, system (16) is described in the following state-space form:

$$x_1'(\hat{t}) - x_1'(\hat{t}-2\hat{\tau}_t) = -x_1(\hat{t}) - x_1(\hat{t}-2\hat{\tau}_t) - x_3(\hat{t}) + x_3(\hat{t}-2\hat{\tau}_t) + \omega(\hat{t}-\hat{\tau}_t), \quad (19a)$$

$$x_2'(\hat{t}) - x_2'(\hat{t}-2\hat{\tau}_a) = -\kappa x_2(\hat{t}) + \kappa x_2(\hat{t}-2\hat{\tau}_a) - \psi x_3(\hat{t}) + \psi x_3(\hat{t}-2\hat{\tau}_a) + v(\hat{t}-\hat{\tau}_a), \quad (19b)$$

$$x_3 = \int_{\hat{t}-\hat{\tau}_0}^{\hat{t}} -\chi x_1(\theta) + x_2(\theta)d\theta, \quad (19c)$$

with $x(\hat{t}) = [x_1, x_2, x_3]^T := \big[\phi'(\hat{t}), u'(\hat{t}), \hat{d}(\hat{t})\big]^T$.

3. CONTROL PROBLEM FORMULATION

The neutral terms in (5), (6), which makes the dynamics dependent on its state at $2\tau_t$ and $2\tau_a$ seconds ago, originates from the elastic waves traveling from the bit to the top of the drill-string and then returning back to the bit. Accordingly, the neutral terms will be removed by preventing the up-traveling wave to be reflected at the top. Based on this notion, a precompensator is designed in Section 3.1 to remove the neutral terms from the equations of motion. Then, a new approach for checking the exponential stability of the dynamics in the compensated coordinates with a prescribed decay rate is developed in Section 3.2. In this approach, which we call the "eigenvector contradiction method", a sufficient condition is presented to ensure that none of the eigenvalues lie in an undesirable right-half complex plane. If there exists an eigenvalue in such half-plane, an eigenvector corresponding to such eigenvalue has to satisfying the corresponding (eigenvalue problem) matrix equation. According to this matrix equation, some inequalities between the magnitudes of the eigenvector elements are extracted. Then, such inequalities are combined to obtain an inequality between the system parameters (and control gains). By choosing control gains in a way that violates such inequality, the existence of an eigenvalue in the undesirable complex half-plane becomes impossible and the stability is guaranteed.

3.1 Compensator design methodology

The up-traveling wave $\dot{\eta}_t(t)$ can be expressed in terms of the measurable velocities and strains at the top by multiplying (3b) by $1/c_t$ and adding it to (3a) as follows:

$$\dot{\eta}_t(t) = \frac{1}{2}\frac{\partial\Phi}{\partial t}(0,t) + \frac{1}{2c_t}\frac{\partial\Phi}{\partial x}(0,t). \quad (20)$$

Accordingly, the up-traveling wave $\dot{\eta}_t(t)$ is available for feedback. On the other hand, solving (3c) and (3d) gives $\dot{\eta}_t(t)$ in terms of down-hole variables as follows:

$$\dot{\eta}_t(t+\tau_t) = \frac{1}{2}\left(\frac{\partial\Phi}{\partial t}(L,t) + \frac{1}{c_t}\frac{\partial\Phi}{\partial x}(L,t)\right). \quad (21)$$

Substituting $\partial\phi/\partial x(L,t)$ from (4a) into (21), regarding $\Phi(L,t) = \Phi_b(t)$, yields:

$$\dot{\eta}_t(t) = \ddot{\Phi}_b(t-\tau_t) - \frac{GJc_t}{J_b}\dot{\Phi}_b(t-\tau_t) + \frac{1}{J_b}T(t-\tau_t). \quad (22)$$

Now, let us introduce the following input transformation to remove the neutral terms from the equations of motion (5) and (6):

$$\Omega_t(t) = \Omega(t) - \dot{\eta}_t(t), \quad V_t(t) = V(t) - \dot{\eta}_a(t), \quad (23)$$

where $\Omega_t(t)$ and $V_t(t)$ are the transformed control inputs with the measurable up-traveling waves $\dot{\eta}_t(t)$ and $\dot{\eta}_a(t)$ as the precompensation terms. By employing such input transformation, the torsional dynamics (5) is transformed, with regards to (22), as follows:

$$\ddot{\Phi}_b(t) = -\frac{GJc_T}{J_b}\dot{\Phi}_b(t) - \frac{1}{J_b}T(t) + \frac{2GJc_t}{J_b}\Omega_t(t-\tau_t). \quad (24)$$

Similarly, the transformed form of the axial dynamics, by application of the input transformation in (23), is obtained as follows:

$$\ddot{U}_b(t) = -\frac{EAc_a}{M_b}\dot{U}_b(t) - \frac{1}{M_b}W(t) + \frac{2EAc_a}{M_b}V_t(t-\tau_a)t. \quad (25)$$

Unlike (5), (6), the transformed system (24), (25) does not include any neutral terms, and hence, its spectrum has no vertical asymptote. The dimensionless perturbation form of the transformed dynamics (24), (25), according to the procedure in subsection 2.2 and subsection 2.1, is obtained as follows:

$$\phi''(\hat{t}) = -\phi'(\hat{t}) - \hat{d}(\hat{t}) + \omega_t(\hat{t} - \hat{\tau}_t), \tag{26a}$$
$$u''(\hat{t}) = -\kappa u'(\hat{t}) - \psi\hat{d}(\hat{t}) + v_t(\hat{t} - \hat{\tau}_a), \tag{26b}$$

where $\omega_t(\hat{t})$ and $v_t(\hat{t})$ are the dimensionless perturbed form of the transformed control inputs (23),

$$\omega = \frac{2GJc_t}{J_b} t_*^2 \Omega_t, \quad v = \frac{2EAc_a}{M_b} \frac{t_*^2}{L_*} V_t. \tag{27}$$

Equations (26) can be described by employing the state vector used in (19) as follows:

$$x_1'(\hat{t}) = -x_1(\hat{t}) - x_3(\hat{t}) + \omega_t(\hat{t} - \hat{\tau}_t), \tag{28a}$$
$$x_2'(\hat{t}) = -\kappa x_2(\hat{t}) - \psi x_3(\hat{t}) + v_t(\hat{t} - \hat{\tau}_a), \tag{28b}$$
$$x_3 = \int_{\hat{t}-\hat{\tau}_0}^{\hat{t}} -\chi x_1(\theta) + x_2(\theta) d\theta, \tag{28c}$$

As a consequence, the proposed precompensation strategy simplifies the dynamics to be stabilized, enabling the stabilizing controller design discussed in subsection 3.2.

3.2 State-feedback control design methodology

Let us define the following state-feedback control law:

$$\omega_t(\hat{t} - \hat{\tau}_t) = -K_1 x(\hat{t}), \quad v_t(\hat{t} - \hat{\tau}_a) = -K_2 x(\hat{t}). \tag{29}$$

Note that this feedback strategy is non-causal and can as such not be implemented directly. It has been shown in Tashakori et al. (2021) that such control strategy can be extended with a predictor to render the total strategy causal and implementable. Here, we refrain from discussing the inclusion of the predictor for the sake of brevity. The gain matrices in (29) are proposed to have the following structure:

$$K_1 = [k_{11}\ 0\ k_{13}], \quad K_2 = [0\ k_{22}\ k_{23}], \tag{30}$$

with k_{11}, k_{13}, k_{22}, k_{23}, the controller gains. These gains are designed to place all poles of the system (28) in the left-half plane $R^-_{-\nu} = \{\lambda | Re(\lambda) \leq -\nu\}$ for an arbitrary positive value ν. Substituting (29) into (28) gives:

$$x_1'(\hat{t}) = (k_{11} - 1)x_1(\hat{t}) + (k_{13} - 1)x_3(\hat{t}), \tag{31a}$$
$$x_2'(\hat{t}) = (k_{22} - \kappa)x_2(\hat{t}) + (k_{23} - \psi)x_3(\hat{t}), \tag{31b}$$
$$x_3(\hat{t}) = \int_{\hat{t}-\hat{\tau}_0}^{\hat{t}} -\chi x_1(\theta) + x_2(\theta) d\theta. \tag{31c}$$

The characteristic matrix of the closed-loop system is then obtained as follows:

$$\Delta_c(\lambda) = \begin{bmatrix} \lambda + 1 - k_{11} & 0 & 1 - k_{13} \\ 0 & \lambda + \kappa - k_{22} & \psi - k_{23} \\ \chi g(\lambda) & -g(\lambda) & 1 \end{bmatrix}, \tag{32}$$

by introducing $g(\lambda) = 1 - e^{\lambda\hat{\tau}_0}/\lambda$.

In the following theorem, we provide analytical and parametric (in the system parameters) synthesis conditions for the controller gains in (29) that ensure the exponential stabilization (with guaranteed exponential convergence rate).

Theorem 1. (Contradiction eigenvalue criterion) If the following relations hold between the control gains and the parameters of the system (31):

$$1 - k_{11}, \kappa - k_{22} > \nu, \quad 1 - k_{13}, \psi - k_{23} > 0 \tag{33a}$$
$$\frac{1 + e^{\tau_0 \nu}}{\nu} \left(\frac{\chi(1 - k_{13})}{1 - k_{11} - \nu} + \frac{\psi - k_{23}}{\kappa - k_{22} - \nu} \right) \leq 1, \tag{33b}$$

then all poles of the system (31) are in the half-plane $R^-_{-\nu} = \{\lambda | Re(\lambda) \leq -\nu\}$.

Proof. Assume that there exists a characteristic root λ_r for the characteristic matrix (32), which belongs to the complex set $R^+_{-\nu} = \{x | Re(x) > -\nu\}$. Correspondingly, there exists a nontrivial eigenvector $V_r = [v_1, v_2, v_3]^T$, which satisfies the following equation:

$$\begin{bmatrix} \lambda_r + 1 - k_{11} & 0 & 1 - k_{13} \\ 0 & \lambda_r + \kappa - k_{22} & \psi - k_{23} \\ \chi g(\lambda_r) & -g(\lambda_r) & 1 \end{bmatrix} \begin{bmatrix} v_1 \\ v_2 \\ v_3 \end{bmatrix} = 0, \tag{34}$$

which gives the following magnitude equalities:

$$|\lambda_r + 1 - k_{11}||v_1| = |1 - k_{13}||v_3|, \tag{35a}$$
$$|\lambda_r + \kappa - k_{22}||v_2| = |\psi - k_{23}||v_3|, \tag{35b}$$
$$|g(\lambda_r)||\chi v_1 - v_2| = |v_3|. \tag{35c}$$

According to Lemma 4 and the triangle inequality, the following inequality can be obtained from (35c):

$$|v_3| \leq |g(\lambda_r)|(\chi|v_1| + |v_2|) \leq \frac{1 + e^{-\hat{\tau}_0 \nu}}{\nu} (\chi|v_1| + |v_2|). \tag{36}$$

Regarding Lemma 3 and condition (33a), the following inequalities are obtained:

$$|\lambda_r + 1 - k_{11}| > 1 - k_{11} - \nu, \tag{37a}$$
$$|\lambda_r + 1 - k_{22}| > 1 - k_{22} - \nu. \tag{37b}$$

Substituting (37) in (35a) and (35b), considering (33a), gives the following inequalities:

$$|v_1| < \frac{1 - k_{13}}{1 - k_{11} - \nu} |v_3|, \quad |v_2| < \frac{\psi - k_{23}}{\kappa - k_{22} - \nu} |v_3|. \tag{38a}$$

Substituting (38) into (36) leads to the following relation:

$$\frac{1 + e^{-\hat{\tau}_0 \nu}}{\nu} \left(\frac{\chi(1 - k_{13})}{1 - k_{11} - \nu} + \frac{\psi - k_{23}}{\kappa - k_{22} - \nu} \right) > 1, \tag{39}$$

which is in contradiction with the condition (33b). As a result, the assumption is not valid, and the theorem is proved by contradiction.

Theorem 1 already gives synthesis conditions for the feedback controllers gains (depending parametrically on drill-string system parameters). However, the controller gains cannot be explicitly designed by the relations in Theorem 1. Now, Proposition 2 gives the controller gains explicitly in terms of the drill-string system parameters, based on the conditions presented in Theorem 1.

Proposition 2. Let d_1, d_2, d_3, and d_4 be arbitrary, positive real numbers, which satisfy

$$1 - d_3 - d_4 > 0. \tag{40}$$

Then, the following control gains ensure that all closed-loop poles in (31) are in the half-plane $R^-_{-\nu} = \{\lambda | Re(\lambda) \leq -\nu\}$:

$$k_{11} = 1 - \nu - d_1, \quad k_{13} = 1 - \frac{d_1 d_3}{\chi \frac{1 + e^{-\hat{\tau}_0 \nu}}{\nu}},$$
$$k_{22} = \kappa - \nu - d_2, \quad k_{23} = \psi - \frac{\nu d_2 (1 - d_3 - d_4)}{1 + e^{-\hat{\tau}_0 \nu}}. \tag{41}$$

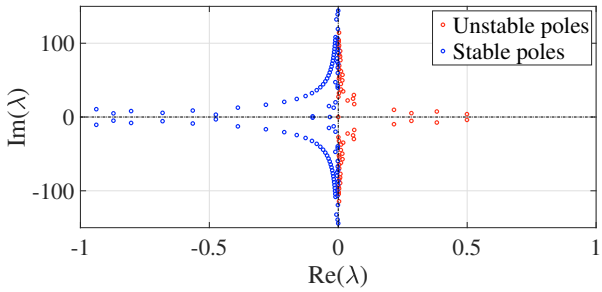

Fig. 1. Open-loop spectrum.

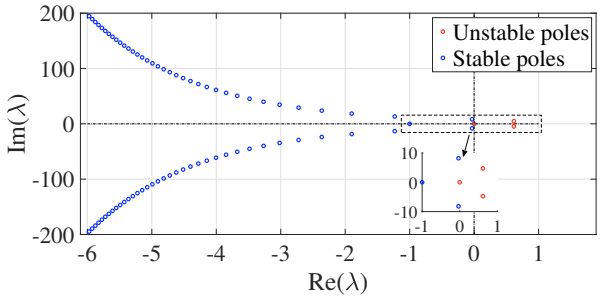

Fig. 2. Open-loop spectrum of the transformed system.

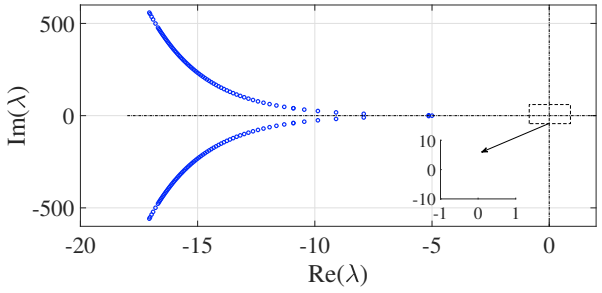

Fig. 3. Closed-loop spectrum.

Proof. Since d_1, d_2, d_3 ,and $1-d_3-d_4$ are positive values, the first condition of Theorem 1, (33a), is satisfied. The following relation is obtained from (41):

$$\frac{1+e^{\tau_0\nu}}{\nu}\left(\frac{\chi(1-k_{13})}{1-k_{11}-\nu}+\frac{\psi-k_{23}}{\kappa-k_{22}-\nu}\right)=1-d_4. \quad (42)$$

According to (40) and the positiveness of d_3 and d_4, the inequality $1-d_4<1$ holds, which indicates the satisfiction of the second condition of (33b) regarding (42).

Compared to the existing approaches for NDDE models, the novel control design method explicitly gives the control gains as functions of the drill-string parameters, which makes it applicable for different drill-strings, needless to redesign the controller.

4. SIMULATION RESULTS

In this section, the effectiveness of the designed controller on the drill-string dynamics (5), (6) is illustrated. Employing the drilling parameters presented in Tashakori et al. (2021) gives the dimensionless parameter values as $\kappa=0.65$, $\psi=13.5$, and $\chi=0.32$.

The open-loop spectrum of the system (with $\Omega(t)=V(t)=0$), which is equivalent to the spectrum of the system (19) with $\omega(\hat{t})=v(\hat{t})=0$, is shown in Fig. 1. The TDS-STABIL MATLAB package Michiels (2010) is employed to find the stability-relevant characteristic roots of the system. The existence of some characteristic roots in the RHP indicates that the system is inherently unstable. As shown, the asymptote of the NTD system (5), (6) is located on the imaginary axis indicating the system is not formally stable, either.

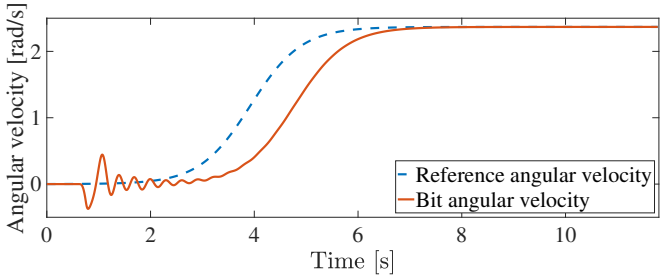

Fig. 4. Reference tracking.

Regarding (23), the control inputs are decomposed into two parts, e.g., $\Omega_t(t)$ and the precompensating part $\dot{\eta}_t(t)$ in the angular direction. First, the precompensating parts $\dot{\eta}_t(t)$ and $\dot{\eta}_a(t)$ are designed by measuring the top-side velocities and strains, see relation (21). Mathematically, the precompensating part can be written in terms of the bit state by using the relation (22). Therefore, the full torsional and axial dynamics (5), (6) with the control inputs $\Omega(t)$, $V(t)$ are transformed into compensated dynamics (24), (25) with the control inputs $V_t(t)$, $\Omega_t(t)$.

The open-loop spectrum of the precompensated dynamics (24), (25) (with $\Omega_t=V_t=0$) is depicted in Fig. 2. Compared to Fig. 1, the number of unstable poles is decreased, and there is no root accumulation. However, still, there are some unstable poles.

The next step is to design the remaining parts of the control inputs $\Omega_t(t)$ and $V_t(t)$ by employing the state-feedback law (29) with regards to (27). Based the eigenvalue contradiction approach, the feedback gains in (29) should be designed by setting the values for d_1, d_2, d_3, and d_4 in (41). By choosing $d_1=d_2=2$, $d_3=0.5$, $d_4=0.1$ (other values satisfying the conditions in Proposition 2 can also be chosen) and the exponential design parameter $\nu=3$ (larger values can be chosen but it increases the sensitivity of the closed-loop system to noise and disturbance), the control gains are designed as follows to exponentially stabilize the system, i.e., to place all roots such that their real values are smaller than $-\nu=-3$:

$$k_{11}=-4,\ k_{22}=-4.35,\ k_{13}=0.72,\ k_{23}=-109.9. \quad (43)$$

The spectrum of the closed-loop system is illustrated in Fig. 3. As shown, all roots have real values less than the intended value -3. Furthermore, the time evolution of the angular velocity of the closed-loop system is illustrated in Fig. 4. Fig. 4 shows that the bit angular velocity approaches the desired trajectory. Employing the smoothened trajectory for the reference values prevents large overshoots at the beginning of the operation. It is seen that the tracking operation is delayed. Such delay is unavoidable according to the input delay corresponding to the time required for the elastic waves to reach the bit.

5. CONCLUSIONS

An automated control scheme has been presented to mitigate undesired vibrations of a distributed drill-string, formulated in terms of NDDEs. By employing a novel precompensator, the open-loop dynamics has been transferred into the RDDE rather than the NDDE framework. A sufficient condition, the eigenvector contradiction criterion, is developed to ensure that the right-most pole is located in a prescribed left-half complex plane. Based on this criterion, a parametric controller is designed in analytic form (depending on drill-string system parameters). Simulation results indicate that the proposed controller stabilizes the drilling system, which is unstable for the selected field parameters, with the prescribed decay rate.

REFERENCES

Aarsnes, U.J.F. and van de Wouw, N. (2018). Dynamics of a distributed drill string system: Characteristic parameters and stability maps. *Journal of Sound and Vibration*, 417, 376–412.

Besselink, B., Vromen, T., Kremers, N., and Van De Wouw, N. (2015). Analysis and control of stick-slip oscillations in drilling systems. *IEEE transactions on control systems technology*, 24(5), 1582–1593.

Boussaada, I., Mounier, H., Niculescu, S.I., and Cela, A. (2012). Analysis of drilling vibrations: A time-delay system approach. In *2012 20th Mediterranean Conference on Control & Automation (MED)*. IEEE.

Bresch-Pietri, D. and Di Meglio, F. (2016). Prediction-based control of linear input-delay system subject to state-dependent state delay-application to suppression of mechanical vibrations in drilling. *IFAC-PapersOnLine*, 49(8), 111–117.

Detournay, E. and Defourny, P. (1992). A phenomenological model for the drilling action of drag bits. In *International journal of rock mechanics and mining sciences & geomechanics abstracts*, volume 29, 13–23. Elsevier.

Faghihi, M.A., Tashakori, S., Yazdi, E.A., and Eghtesad, M. (2022). Multiple regenerative effects of the bit-rock interaction in a distributed drill-string system. In *10th International Conference on Wave Mechanics and Vibrations (WMVC)*.

Germay, C., Denoël, V., and Detournay, E. (2009). Multiple mode analysis of the self-excited vibrations of rotary drilling systems. *Journal of Sound and Vibration*, 325(1-2), 362–381.

Krstic, M. (2009). Delay compensation for nonlinear, adaptive, and pde systems.

Loiseau, J.J., Cardelli, M., and Dusser, X. (2002). Neutral-type time-delay systems that are not formally stable are not bibo stabilizable. *IMA Journal of Mathematical Control and Information*, 19(1_and_2), 217–227.

Michiels, W. (2010). Tds stabil: A matlab tool for fixed-order stabilization problems for time-delay systems.

Priest, J., Ghadbeigi, H., Avar-Soberanis, S., and Gerardis, S. (2021). 3d finite element modelling of drilling: The effect of modelling method. *CIRP Journal of Manufacturing Science and Technology*, 35, 158–168.

Richard, T., Germay, C., and Detournay, E. (2007). A simplified model to explore the root cause of stick–slip vibrations in drilling systems with drag bits. *Journal of sound and vibration*, 305(3), 432–456.

Saldivar, B., Mondié, S., Loiseau, J.J., and Rasvan, V. (2013). Suppressing axial-torsional coupled vibrations in drillstrings. *Journal of Control Engineering and Applied Informatics*, 15(1), 3–10.

Tashakori, S. and Fakhar, M. (2019). Suppression of torsional vibrations in drilling systems by using the optimization-based adaptive backstepping controller. *Int. J. Mech. Control*, 20(1), 105–110.

Tashakori, S., Vossoughi, G., Zohoor, H., and van de Wouw, N. (2021). Prediction-based control for mitigation of axial–torsional vibrations in a distributed drill-string system. *IEEE Transactions on Control Systems Technology*, 30(1), 277–293.

Tashakori, S., Vossoughi, G., Zohoor, H., and Yazdi, E.A. (2020). Modification of the infinite-dimensional neutral-type time-delay dynamic model for the coupled axial–torsional vibrations in drill strings with a drag bit. *Journal of Computational and Nonlinear Dynamics*, 15(8).

Vromen, T., Dai, C.H., van de Wouw, N., Oomen, T., Astrid, P., Doris, A., and Nijmeijer, H. (2017). Mitigation of torsional vibrations in drilling systems: A robust control approach. *IEEE Transactions on Control Systems Technology*, 27(1), 249–265.

Appendix A

Lemma 3. For positive values $b > \nu > 0$, $min|\lambda+b|_{\lambda\in D} = b-\nu$, where $D = \{\lambda | Re(\lambda) \geq -\nu\}$.

Proof. Since $Re(\lambda) \geq -\nu$, we can write $Re(\lambda) = -\nu + \alpha + \beta i$ where α is a non-negative real number, and β is a real number. Hence, for $\lambda \in D$,

$$|\lambda+b| = \sqrt{\big(Re(\lambda)+b\big)^2 + Im(\lambda)^2} = \sqrt{(b-\nu+\alpha)^2+\beta^2}, \tag{A.1}$$

where $min\sqrt{(b-\nu+\alpha)^2+\beta^2}_{\alpha\geq 0,\beta} = b-\nu$, which completes the proof of the statement of the lemma.

Lemma 4. The maximum magnitude of the complex function $g(\lambda) = (1-e^{\lambda\hat{\tau}_0})/\lambda$ in the region $D = \{\lambda | Re(\lambda) \geq -\nu\}$, with $\hat{\tau}_0, \nu > 0$, is not greater than $(1+e^{-\hat{\tau}_0\nu})/\nu$.

Proof. Let us divide the region D into two sub-regions, inside and outside the ball $|\lambda| = \nu$: $D_1 = \{\lambda | |\lambda| \leq \nu\}$, and $D_2 = \{\lambda | Re(\lambda) > -\nu \wedge |\lambda| > \nu\}$, respectively. Since $\lim_{\lambda\to 0} g(\lambda) = -\hat{\tau}_0$, the origin is a removable singular point for $g(\lambda)$, and the function $g(\lambda) = (1-e^{\lambda\hat{\tau}_0})/\lambda$, (with defining $g(0) = -\hat{\tau}_0$) can be considered as an analytic function. Hence, according to the maximum modulus principle in complex analysis, its maximum magnitude in the region D_1 corresponds to a point located on its boundary, $|\lambda| = \nu$:

$$\begin{aligned} max|\frac{1-e^{\lambda\hat{\tau}_0}}{\lambda}|_{\lambda\in D_1} &= max|\frac{1-e^{\lambda\hat{\tau}_0}}{\lambda}|_{|\lambda|=\nu} \\ &\leq \frac{1+max|e^{\lambda\hat{\tau}_0}|_{|\lambda|=\nu}}{\nu} = \frac{1+e^{\nu\hat{\tau}_0}}{\nu}. \end{aligned} \tag{A.2}$$

In addition, $inf|\lambda|_{\lambda\in D_2} = \nu$ and since $sup\big(Re(-\lambda\hat{\tau}_0)\big) = \nu\hat{\tau}_0$, $sup|e^{-\lambda\hat{\tau}_0}|_{\lambda\in D_2} = e^{\nu\hat{\tau}_0}$, the following relation holds:

$$sup|\frac{1-e^{\lambda\hat{\tau}_0}}{\lambda}|_{\lambda\in D_2} \leq \frac{1+sup|e^{\lambda\hat{\tau}_0}|_{\lambda\in D_2}}{\nu} = \frac{1+e^{\nu\hat{\tau}_0}}{\nu}. \tag{A.3}$$

As a result, $max|\frac{1-e^{\lambda\hat{\tau}_0}}{\lambda}|_{\lambda\in D} \leq \frac{1+e^{\nu\hat{\tau}_0}}{\nu}$.